THE SSME HPFTP WAVY INTERSTAGE SEAL: PART II — ROTORDYNAMIC ANALYSIS

B. T. Murphy, J. K. Scharrer, and L. A. Hawkins
Rockwell International, Rocketdyne Division
Canoga Park, California

ABSTRACT

In Part I, an analysis was presented for the calculation of rotordynamic coefficients for the SSME HPFTP impeller interstage seals having wavy solid boundaries (i.e., nonlinear clearance functions). This is a significant extension beyond prior analyses which considered only straight and/or tapered seal boundaries. Part II presents the detailed rotordynamic analysis of the SSME HPFTP, and quantifies the effect of the seal analysis refinement on the rotordynamics. Results are presented for both the linearized stability model of the turbopump as well as nonlinear steady state response simulations. The nonlinear studies involve a combination of low level parametrically-excited and self-excited subsynchronous rotor motion closely resembling actual hot fire accelerometer and displacement data. Direct comparisons are made for the current interstage seal hardware employing equally smooth rotor and stator surfaces, as well as a set of new knurled seals scheduled for engine testing in 1989.

NOMENCLATURE

DN	Bearing Diameter times shaft speed (N)
FMOF	First Manned Orbital Flight
FPL	Full Power Level
FWR	Front Wear Ring seal
Grms	Acceleration (G) root mean square
HPFTP	High Pressure Fuel Turbopump
OSI	Onset Speed of Instability
RWR	Rear Wear Ring seal
SSME	Space Shuttle Main Engine
SSV	Subsynchronous Vibration

INTRODUCTION

The Space Shuttle Main Engine High Pressure Fuel Turbopump (SSME HPFTP, see Figure 1) is one of the most exotic pieces of turbomachinery ever built [Rothe, 1974]. Its rotating assembly weight of only 578 N (130 lbs), combined with a maximum rating of 57.4 MW (77,000 hp), easily gives it one of the highest power-to-weight ratios for any class of rotating machinery. Table 1 shows some of the more significant operating parameters associated with the Full Power Level rating (FPL).

The turbopump consists of three identical pump stages driven on a common built-up shaft by a two stage turbine. The shaft is supported radially by two pairs of preloaded duplex bearings. All four bearings have 45 mm bores, and operate at a DN (bearing bore in mm times shaft speed in rpm) in excess of 1.6 million. The outer race of each bearing can slide axially in its housing to accommodate shaft growth/contraction and small amounts of axial travel brought on by changes in thrust balance. Transient thrust imbalances experienced during start-up and shut-down are reacted by an additional mechanical bearing at the pump end of the shaft. During mainstage operation (>12,000 cpm (rpm)) this bearing lifts off as a balance piston, integral with the third stage pump impeller, becomes active.

The turbopump has a pair of high-pressure interstage seals located between the 1st and 2nd stage pump impellers and the 2nd and 3rd stage pump impellers. The influence of these seals on the rotordynamics of the turbopump is appreciable [Childs, 1973, 1978, Ek, 1980]. To date, the rotordynamic coefficients for annular seals had been based on straight and/or tapered solid boundaries. In Part I, an incompressible flow seal analysis was presented which extends the current state-of-the-art to permit wavy boundaries (i.e., as nonlinear clearance functions). This extension is significant because the current SSME HPFTP seal hardware, which was designed to be straight, undergoes considerable deformation due to pressure, temperature, speed and stack-up preload effects. In Part I, these deformations were shown to be about 30% of the nominal radial clearance.

The purpose of this paper is to show what effect the seal analysis refinement has on the rotordynamics of the SSME

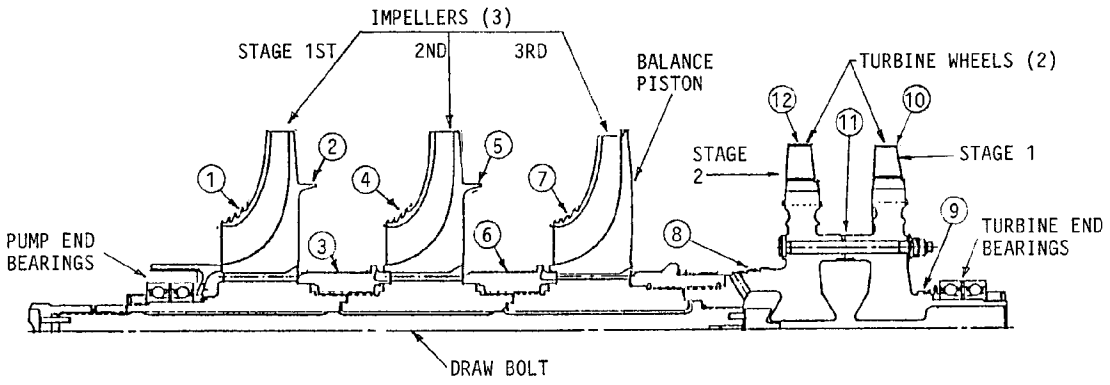

Fig. 1. Half Cross Section of High-Pressure Fuel Turbopump.

Table 1. FPL Operating Parameters for SSME HPFTP

Rotating Speed	36,600 cpm	36,600 rpm
Pump Flow Rate	67,000 lpm	17,000 gpm
Pump Inlet Pressure	23.5 Bar	341 psi
Pump Discharge Pressure	482 Bar	6,990 psi
Turbine Inlet Temperature	994 K	1,790 °R
Turbine Inlet Pressure	338 Bar	4,900 psi
Power	57.4 MW	77,000 HP

HPFTP, and thereby underscore its relevance. This is done with the linearized stability model of the turbopump and with nonlinear steady state response simulations. The focus of the nonlinear simulations is on subsynchronous vibrations, which are due to a combination of parametrically excited forced response and self-excited limit cycles of the rotor's first natural mode of vibration.

ROTORDYNAMIC MODEL

The linear elastic model of the rotating assembly (shown in Figure 2) is comprised of cylindrical and tapered finite element beam elements. There are 73 elements in the rotor model, with 78 nodes having 4 degrees of freedom per node. The mass distribution of the rotor is modeled with translational and diametral inertias lumped at 24 of the 78 nodes.

The degrees of freedom with no assigned inertia are statically condensed out of the global stiffness matrix [Zienkiewicz, 1977]. The resulting mass-elastic rotor model has a total of 72 degrees of freedom. The undamped free-free bending modes computed with this model are shown in Table 2, along with results from free-free modal tests performed on a complete rotor assembly (model material properties and other pertinent inputs reflect the ambient conditions of the modal test). Correlation of the first two modes is as expected and meets requirements. The measured shape of the third mode indicates that the onset of disk flexibility effects is primarily responsible for the test frequency being significantly lower than predicted. This level of discrepancy is acceptable, however, as the mode is far enough removed from the frequency range of operation. The undamped free-free modes for the rotor reflecting operating conditions were used for all rotordynamic analyses for

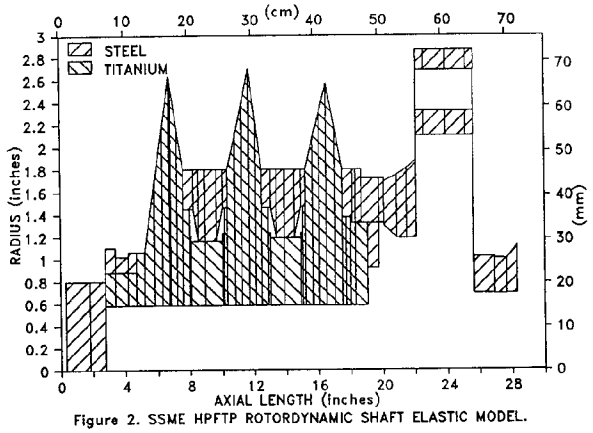

Figure 2. SSME HPFTP ROTORDYNAMIC SHAFT ELASTIC MODEL.

the turbopump employing modal synthesis techniques [Craig, 1981].

At the modal synthesis stage the modes of the rotor are coupled to modes obtained from a grounded housing finite element model. The housing model has 23 master degrees of freedom, and the lowest 18 bending modes were used ranging from 50 Hz to 2757 Hz. All other facets of the rotordynamic model are then introduced at this point. For the linear (eigenvalue) stability model these include:

1. linearized ball bearing stiffnesses,
2. pump interstage seal stiffness and damping,
3. pump impeller forward and rear wear ring seals stiffness and damping,
4. turbine interstage labyrinth seal stiffness and damping,
5. aerodynamic cross coupling for each turbine stage (Alford's Force),
6. pump impeller dynamic coefficients were assumed negligible, and
7. rotor gyroscopic effects.

Table 2. Rotating Assembly Free-Free Modes

Mode Number	Test Freq.(Hz)	Anal. Freq.(Hz)	Percent Difference
1	574	594	+3%
2	1104	1104	0%
3	1473	1607	+9%

All the above elements are defined throughout the turbopump operating speed range using the appropriate computer codes. Ball bearing stiffnesses are obtained from load deflection curves computed with an industry standard quasi-static rolling element bearing program by Jones [1960]. The bearing stiffness is then combined in series with a bearing support stiffness before input to the rotordynamic model. The relatively small rotordynamic coefficients for the impeller wear ring seals and turbine interstage seals were estimated according to the short seal analysis of Childs [1983]. Both turbine stages are not shrouded, and the load split between them is 50/50, so experience dictates that the aerodynamic cross-coupling be based on an efficiency factor of $\beta = 1.5$[Alford, 1965]. Table 3 lists these coefficients for the FPL rating.

In the nonlinear simulation model the equations of motion are integrated numerically with time to yield steady state responses. Because of the on/off nature of some of the nonlinearities, all results reported here employed first order integration schemes with a time step of about 0.000012 seconds. In addition to all elements of the linear eigenvalue model mentioned above, the elements of the nonlinear model consist of the following:

1. bearing deadband for ball bearings nominally .00635 mm (.00025 in), radial,
2. nonlinear load deflection curve for ball bearings (stiffening),
3. static hydrodynamic side load at 3rd stage impeller, 5520 N (1241 lb) at an angle of
70 degrees from the engine flushpar,
4. static aerodynamic side load at 2nd stage turbine, 4400 N (989 lb) at an angle of 0
degrees from the engine flushpar,
5. fixed and rotating (i.e., housing and shaft) eccentricities at pump interstage seals,
6. fixed eccentricities at turbine end ball bearings,
7. unbalances at all pump impellers and turbine disks,
8. rubbing clearance at 2-3 pump interstage seal,
9. rubbing clearance at turbine interstage seal, and
10. rubbing clearance at 3 step labyrinth seal (no. 8 in Figure 1).

Item 2 above is provided by the rolling element analysis computer program (Jones, 1960). Item 5 above is due to machining and assembly tolerances of housing and shaft seal hardware. Item 6 above is similar to item 4 above and is due to a nonuniform circumferential pressure distribution within the turbine discharge duct. Item 7 above has essentially an arbitrary distribution but is limited to an overall net static unbalance of 1 gm-in due to a low speed in-housing trim balance performed after final assembly. Items 8, 9, and 10 above are included in the nonlinear model, but seal rubbing was not present in any simulations reported here.

INTERSTAGE SEAL MODEL

The rotordynamic coefficients of the annular pump interstage seals form the basis of this paper. Since the pressure drops across these two seals are on the order of 149 bar (2165 psi) each, their treatment is critical to obtaining the most relevant rotordynamic model possible. The design of these seals has evolved throughout the SSME development program. Originally, these seals were three stepped labyrinth with teeth on rotor, then three stepped and smooth, and are presently straight and smooth (Figure 3). A straight seal with a rough

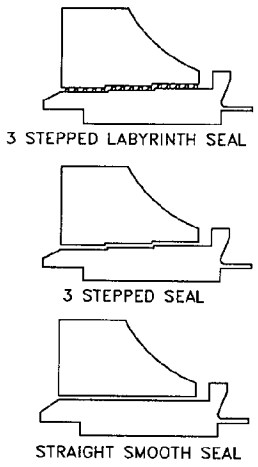

FIGURE 3. VARIOUS INTERSTAGE SEAL CONFIGURATIONS

Table 3. Rotordynamic Coefficients for Elements (except Interstage Seals)

	Kxx	Kxy	Cxx
Ball Bearing	370,000		
1st Stage Imp. FWR+RWR	45,000	5,000	2.7
2nd Stage Imp. FWR+RWR	29,000	4,600	2.5
3rd Stage Imp. FWR	7,700	1,500	0.0
Turbine Interstage Seal	3,300	2,800	1.5
Alford's(each turb. stage)		18,700	

(knurled) stator is also currently being manufactured for possible engine testing in late 1989. Early in the SSME program the stiffness and damping coefficients for the interstage seals were based on the work of Black and Jenssen [1970]. Later these coefficients were updated to the short seal bulk flow model of Childs [1983]. This was then followed by the finite length analysis of Childs and Kim [1985] anchored with experimental results from a high Reynold's number test facility. In all these prior analyses the flow path through the seal was assumed to be straight or, at most, tapered. That is, only linear clearance functions (along the seal axis) were considered. In the case of the SSME HPFTP, all flightweight hardware has been designed and manufactured to be as light as possible. When combined with extremely high internal pressures, high centrifugal forces, large differences between manufacturing-to-assembly-to-operation temperatures, and a large temperature dependent axial stack-up load, the result is interstage seal clearances which are highly nonlinear (Figure 4).

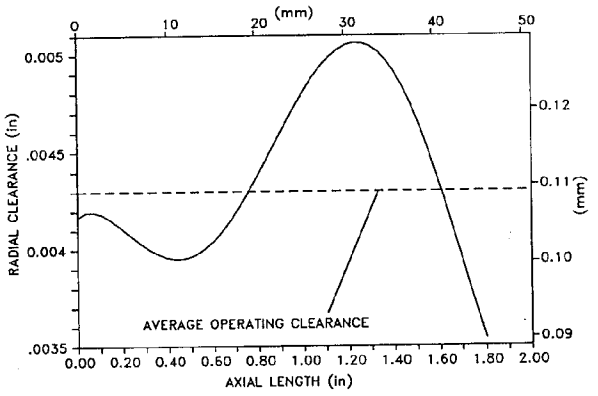

Figure 4a. SSME HPFTP first interstage seal radial clearance.

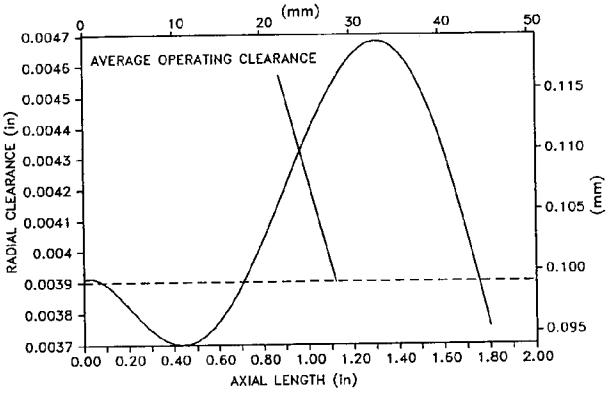

Figure 4b. SSME HPFTP second interstage seal radial clearance.

In Part I, the finite length seal analysis of Childs and Kim was extended to treat nonlinear clearance functions. This was done by re-deriving the seal flow equations for general clearances as opposed to applying the linear clearance analysis in sequence to a piecewise linear representation of the clearance. Figures 5 compare both versions of stiffness and damping coefficients. Note from Figure 4 that the average radial at operation clearance is now about 0.109 mm (0.0043 in) for the 1-2 seal and about 0.099 mm (0.0039 in) for the 2-3 seal, as opposed to 0.140 mm (0.0055 in) for the straight seal. This, along with new terms in the flow equations presented in Part I, is responsible for the significant differences in the coefficients.

Also shown in Figures 5 are the rotordynamic coefficients for the set of wavy knurled seals. These types of seals (i.e., damper seal [von Pragenau, 1982]) are being considered because they offer increased direct damping.

ANALYSIS RESULTS - LINEAR STABILITY MODEL

The primary focus in the linear model is the natural frequency and logarithmic decrement of the first rotor mode as a function of running speed. From this, the onset speed of

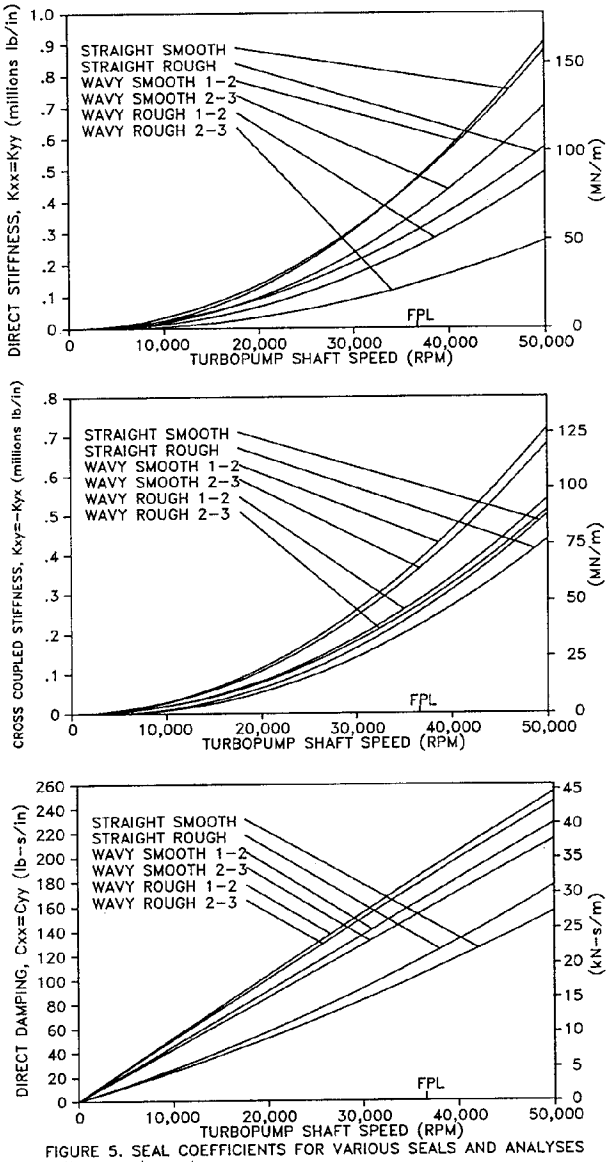

FIGURE 5. SEAL COEFFICIENTS FOR VARIOUS SEALS AND ANALYSES

instability (OSI) is obtained as the speed above which the logarithmic decrement is negative. For the original three stepped labyrinth seal design the OSI was predicted to be about 20,000 rpm (see, for example, Childs [1978]). Early engine testing in 1977 verified this prediction when extremely large and destructive subsynchronous whirling was experienced at the frequency of the first rotor mode. Operation at rated power level (100%) was not possible.

With the three stepped smooth seals the predicted OSI was increased to about 40,000 rpm. Additional stiffness in the ball bearing support structures was also an important contributor to this increase. Subsequent engine testing confirmed these predictions as it was then possible to operate up to full power level (109%).

Manufacturing and assembly tolerances combined with occasional seal rubbing sometimes permitted the subsynchronous whirl to recur during engine testing. Because of the range of these unit to unit variations, the pump was considered only marginally stable at full power level. Also, stability predictions were relatively sensitive to changes in turbine aerodynamic cross coupling. Thus, the additional modification to employ the straight smooth interstage seal was enacted. The OSI in this case is predicted to be greater than 50,000 rpm. Many model parameters are not valid beyond 50,000 rpm, so the actual value is not relevant. Engine test results with the straight smooth seal has shown a definite decrease in the amplitude of subsynchronous vibration as detected with external housing accelerometers. However, the percentage of turbopumps which displayed detectable levels was only slightly less (Table 4).

Engine test experience has indicated that subsynchronous vibration with straight smooth seals, although not desirable, is not harmful. Reviews of post test hardware conditions for straight smooth units have not found any discernible differences between units which displayed subsynchronous vibration and those that did not.

When updating to the wavy seal analysis, the predicted OSI is still greater than 50,000 rpm as with the straight smooth seal. Thus, it is necessary to look at a complete stability map to assess the effect. Figure 6 shows the logarithmic decrement versus running speed for the two sets of smooth seal coefficients. Results are mixed. With the wavy analysis the pump is predicted to be less stable at the low end of the steady state operating speed range, but is unchanged at the high end. Since subsynchronous vibration is now only experienced at higher power levels, updating to the wavy seal coefficients for the smooth seal does not change the results of linear rotordynamic stability model.

As part of an ongoing effort to improve and upgrade the rating of the SSME, a knurled interstage seal stator (or so called "damper seal") is currently being fabricated for possible engine testing in 1989. The increased direct damping of this type of seal has been predicted to further enhance the stability of the turbopump. Figure 6 shows the predicted log decs for the straight knurled seal (based on the old seal analysis). Compared to the straight smooth seal predictions, enhanced stability would be expected throughout the operating speed range. When using the new wavy seal analysis; however, going from smooth to knurled is not such an obvious improvement (Figure 6). The log dec curve for the wavy smooth seal takes on the appearance of having been moved up and to the right by the knurled stator. The log dec is now significantly higher through most of the operating range, but is about the same near max power level. For power levels above about 104% the log dec is actually predicted to be less with the wavy knurled seal. As a means to further assess the knurled seal at full power level, the nonlinear rotordynamic model was used.

ANALYSIS RESULTS - NONLINEAR SIMULATION MODEL

Subsynchronous vibration experienced during engine testing with the straight smooth seal has been primarily at 50% of shaft speed. Percentages as low as 47% and as high as 52% have occurred, but 50% is the norm. A number of references [Ehrich, 1966 and 1967, Bently 1979, Childs 1981] have addressed the issue of 50%, or half-speed, whirl caused by bearing deadband. Essentially, if the static bearing deflections due to static side loads and the synchronous bearing deflections due to mass and seal eccentricities are such that the rotor orbits through the deadband, then half-speed vibration is possible. One of the necessary conditions for this phenomena is that the frequency of the first rotor mode be just above the 50% frequency (as is the case here). Mathematically this subsynchronous vibration is a forced response of a nonlinear system to synchronous excitation, and will be at exactly 50% of shaft speed. The momentary softness experienced when passing through the deadband drops the frequency of the first mode and allows it to tune to 50% of shaft speed [Bently 1979,

Table 4. Occurence of Subsynchronous Vibration with the Three Stepped and Straight Smooth Seals

Seal Type	# Units Tested*	# Units W/S.S.V.	%	Avg. S.S.V. Amplitude	Avg. Synch. Amplitude
Three Step	63	13	21%	5.1 Grms	5.9 Grms
Str. Smooth	70	12	17%	1.2Grms	4.9Grms

* This group of units has similar hardware characteristics in that they all have the same turbine discharge turnaround duct (FMOF) which generates the same aerodynamic static side load on the turbopump shaft.

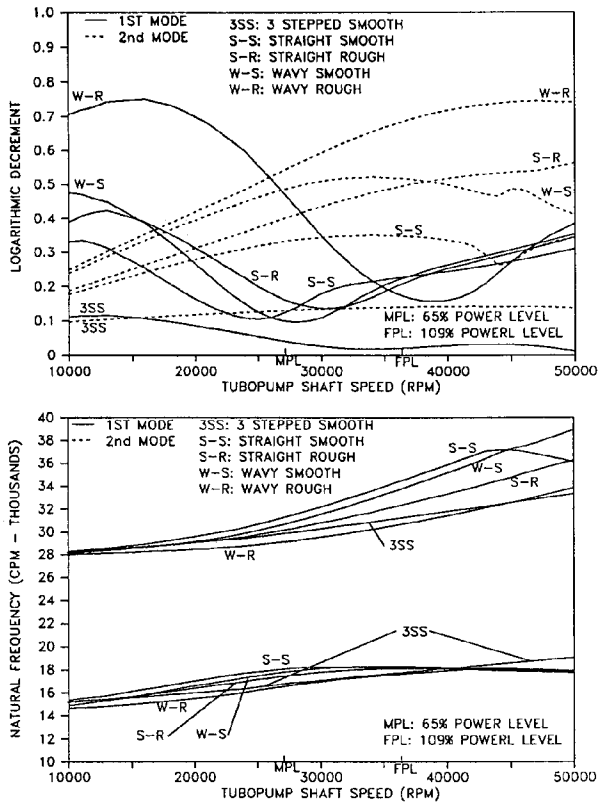

FIGURE 6. NATURAL FREQUENCY AND LOGARITHMIC DECREMENT OF FIRST 2 ROTOR MODES VS. SHAFT SPEED FOR VARIOUS SEALS & ANALYSES.

Childs 1981]. The Rocketdyne nonlinear model can easily be made to exhibit this phenomena by adjusting the eccentricities and bearing deadband (all well within expected tolerance bands).

In the majority of cases subsynchronous vibration in engine test data is at 50% of shaft speed. For those cases which involve power level changes, the vibration tracks shaft speed, maintaining the 50% ratio. For cases where the vibration is at other than 50%, it has been hypothesized that it is a limit cycle whirl of the first rotor mode. That is, as the rotor passes through the bearing deadband it is momentarily unstable in a linear sense due to the momentary lack of bearing stiffness. Stability then returns upon exiting the deadband. In a way analogous to the half speed vibration described above, if conditions are just right, a sustained self excited steady state vibration of the first rotor mode can exist. Its amplitude is inherently self limited since a large amplitude motion spends proportionately less time in the deadband, and thus will have insufficient impetus to be sustained. This type of motion has also been simulated with the nonlinear rotordynamic model. To achieve this, however, it was found necessary to lower the log dec of the first rotor mode by altering the bearing and interstage seal coefficients. Changes to the coefficients on the order of 5% to 10%, in addition to reducing the static side loads by 25%, were necessary to bring on the limit cycle whirl. These changes reduced the log dec by about half, while still maintaining an OSI greater than 50,000 rpm.

Numerous studies of HPFTP subsynchronous vibration behavior have been conducted employing both the half speed and limit cycle whirl models. Standard approach is to adjust mass and seal eccentricities to match observed synchronous and subsynchronous housing acceleration levels for a given test of a particular HPFTP unit. Then use that model as a basis for parameter changes to study a particular effect. For the present paper, SSME HPFTP unit number 2223 was used, having displayed 4.0 Grms of synchronous vibration and 1.6 Grms of 50% subsynchronous vibration at 109% power level. Figure 7 shows typical results employing the deadband interaction mechanism, in this case comparing predicted acceleration amplitudes as a function of bearing deadband for three different sets of interstage seal coefficients. The figure shows that updating the seal analysis for the current straight smooth seal has little effect on the synchronous amplitude and decreases the subsynchronous amplitude. Note that this is not an improvement to be realized, but simply a refinement in the analysis. The model could be readjusted to again have the same levels of synchronous and subsynchronous vibration. The predicted acceleration levels with the knurled seals do indicate, however, that there should be a definite improvement when switching to the new damper seal hardware. The synchronous amplitude is predicted to be less, and in this case the subsynchronous vibration is completely suppressed. The general conclusion drawn from all studies performed with both subsynchronous vibration mechanisms is that both synchronous and subsynchronous amplitudes will be significantly less with the new damper seal.

CONCLUSIONS

The refinement in the analysis of the annular interstage seals was found not to significantly affect the predicted rotordynamic behavior of the SSME HPFTP when employing the current straight smooth interstage seals. When assessing the upcoming hardware change from smooth to knurled seals, however, the new analysis technique was found to have an effect. With the old seal analysis the linear stability model predicted a significant stability improvement with the knurled

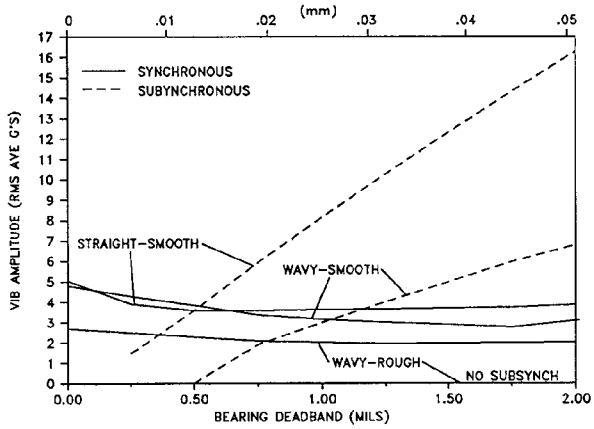

FIGURE 7. Nonlinear response vs. deadband for 3 different seal configurations.

seal hardware. With the new seal analysis, however, the linear stability model predicts no significant change. Use of the nonlinear rotordynamic simulation model was necessary to properly assess the seal hardware change. This was done by investigating the effect on predicted subsynchronous vibration levels when switching seals. In all studies performed, the knurled seals were found to result in lower predicted synchronous and subsynchronous response amplitudes. Thus, the new seal analysis technique did affect the way in which the rotordynamic assessment was done, but did not not change the final result.

REFERENCES

Alford, J. S., 1965, "Protecting Turbomachinery From Self-Excited Rotor Whirl," *ASME Journal of Engineering for Power,*pp. 333-344.

Bently, D., 1979, "Forced Subrotative Speed Dynamic Action of Rotating Machinery," ASME Paper 74-PET-16, Petroleum Mechanical Engineering Conference, Dallas, Texas.

Black, H. F., Jensen, D. N., 1970, "Dynamic Hybrid Bearing Characteristics of Annular Controlled Leakage Seals and Pressure Seals," *Proceedings of the Institution of Mechanical Engineers,* Vol, 184, Pt. 3N, pp. 92-100.

Childs, D. W., 1973, "Transient Rotordynamic Analysis for the Space Shuttle Main Engine High-Pressure Turbopumps," 1973 ASEE-NASA Summer Faculty Fellowship Program Final Report, University of Alabama.

Childs, D. W., 1978, "The Space Shuttle Main Engine High-Pressure Fuel Turbopump Rotordynamic Instability Problem," *ASME Journal of Engineering for Power,* Vol. 100, pp. 48-57.

Childs, D. W., 1981, "Fractional-Frequency Rotor Motion Due to Nonsymmetric Clearance Effects," *ASME Journal of Engineering for Power,* Paper No. 81-GT-145.

Childs, D. W., 1983, "Dynamic Analysis of Turbulent Annular Seals Based on Hir's Lubrication Equation," *ASME Journal of Lubrication Technology,* Vol. 105, No. 3, pp. 437-445.

Childs, D. W., Kim, C., 1985, "Analysis and Testing for Rotordynamic Coefficients of Turbulent Annular Seals With Different, Directionally-Homogeneous Surface-Roughness Treatment for Rotor and Stator Elements," *ASME Journal of Tribology,* Vol. 107, pp. 296-306.

Craig, R. R., 1981,*Structural Dynamics,*John Wiley and Sons, New York.

Ehrich, F. F., 1966, "Subharmonic Vibrations of Rotors in Bearing Clearance," ASME Paper 66-MD-1, Design Engineering Conference and Show, Chicago, Illinois.

Ehrich, F.F., O'Conner, J.J., 1967, "Stator Whirl with Rotors in Bearing Clearances," *ASME Journal of Engineering for Industry,* pp. 381-390.

Ek, M. C., 1980, "Solving Subsynchronous Whirl in the High-Pressure Hydrogen Turbomachinery of the SSME," *J. Spacecraft,*Vol. 17, No. 3, pp. 208-218.

Jones, A. B., 1960, "A General Theory for Elastically Constrained Ball and Radial Roller Bearings Under Arbitrary Load and Speed Conditions," *ASME Journal of Basic Engineering,*Vol. 82, p. 309.

Rothe, K., 1974, "Turbopump Configuration Selection for the Space Shuttle Main Engine," ASME Paper 74-FE-23, Joint Fluid Engineering Conference, Montreal, Canada.

von Pragenau, G. L., 1982, "Damping Seals for Turbomachinery," NASA Technical Paper 1987.

Zienkiewicz, O.C., 1977, *The Finite Element Method,* McGraw-Hill, New York.